Hindawi
International Journal of Analytical Chemistry
Volume 2022, Article ID 7602992, 13 pages
https://doi.org/10.1155/2022/7602992

*Research Article*

# Pharmacokinetic Difference of Six Active Constituents of Huangqi Liuyi Decoction between Control and Diabetic Nephropathy Mouse Models

**Qun Wang**,[1] **Ya Shi**,[1] **Xingde Liu**,[1] **Ting Liu**,[2] **Yongjun Li**,[2] **Xinli Song**,[1] **Xiaolan Chen**,[1] **Yang Jin**,[2] **Wen Liu**,[1] **Yonglin Wang**,[2] **and Zipeng Gong**[2]

[1]*Guizhou University of Traditional Chinese Medicine, Huaxi University Town, Guiyang 550025, China*
[2]*Guizhou Provincial Key Laboratory of Pharmaceutics, Guizhou Medical University, Beijing Road, Guiyang 550000, China*

Correspondence should be addressed to Wen Liu; liuwen0306@163.com, Yonglin Wang; gywyl@gmc.edu.cn, and Zipeng Gong; gzp4012607@126.com

Received 29 November 2021; Accepted 3 May 2022; Published 25 May 2022

Academic Editor: Adil Denizli



Huangqi Liuyi decoction is a famous traditional Chinese medicine (TCM) that has been widely used in China for the management of diabetes since the Song Dynasty. Today, it is commonly used for treating diabetic nephropathy (DN). Our previous experimental studies have suggested that the mixture HQD, containing astragalus saponin, astragalus flavone, astragalus polysaccharide, and glycyrrhetinic acid, could be used for the treatment of DN and to improve renal function. The objective of this study was to develop a sensitive and reliable high-performance liquid chromatography-tandem mass spectrometry method for simultaneous quantitation of astragaloside IV, calycosin-7-O-$\beta$-D-glucoside, calycosin-glucuronide, ononin, formononetin, and glycyrrhizic acid, which are the main active constituents in HQD, and to compare the pharmacokinetics of these active constituents in control and DN mice orally treated with HQD. The results indicated that the pharmacokinetic parameters of HQD were significantly different between the control and DN mouse groups. The absorption of HQD in the DN mice was greater than that in control mice.

## 1. Introduction

Diabetic nephropathy (DN), one of the most serious complications of diabetes mellitus, is an irreversible, progressive disease characterized by a continuous decline in the glomerular filtration rate, proteinuria, microalbuminuria, and increased blood pressure [1–3], with most cases eventually progressing to end-stage renal disease [4]. Prevention of or early treatment for DN may improve the survival rate and quality of life for patients, which would help to avoid the extremely high costs of renal treatment for end-stage renal disease as well as for other complications [5]. Traditional Chinese medicines (TCMs) have been widely applied in the clinical treatment of various diseases for a long time [6]. In particular, TCMs offer unique advantages in the prevention of diabetic complications because of limited side effects and/or less toxicity [7, 8]. Huangqi Liuyi decoction (HQD) is a popular TCM formula that has been used in China since the Song Dynasty. It is composed of *Radix Astragali* and *Radix Glycyrrhizae*. Research has shown that HQD can significantly decrease the fasting blood glucose and improve the degree of pathological damage to the kidneys in DN rats [9, 10]. In preliminary pharmacodynamic research work of our research group, the results confirmed that the main active components of HQD for the treatment of DN are astragalus saponin, astragalus flavone, astragalus polysaccharide, and glycyrrhizic acid, and the mixture of these four active components (HQD) can significantly delay the pathogenesis of DN in db/db mice. Moreover, the difference in pharmacodynamics was not statistically significant between HQD and Huangqi Liuyi decoction.

In recent years, an increasing amount of research has shown that the pharmacokinetic parameter of traditional Chinese medicine can be affected by the disease states [11].

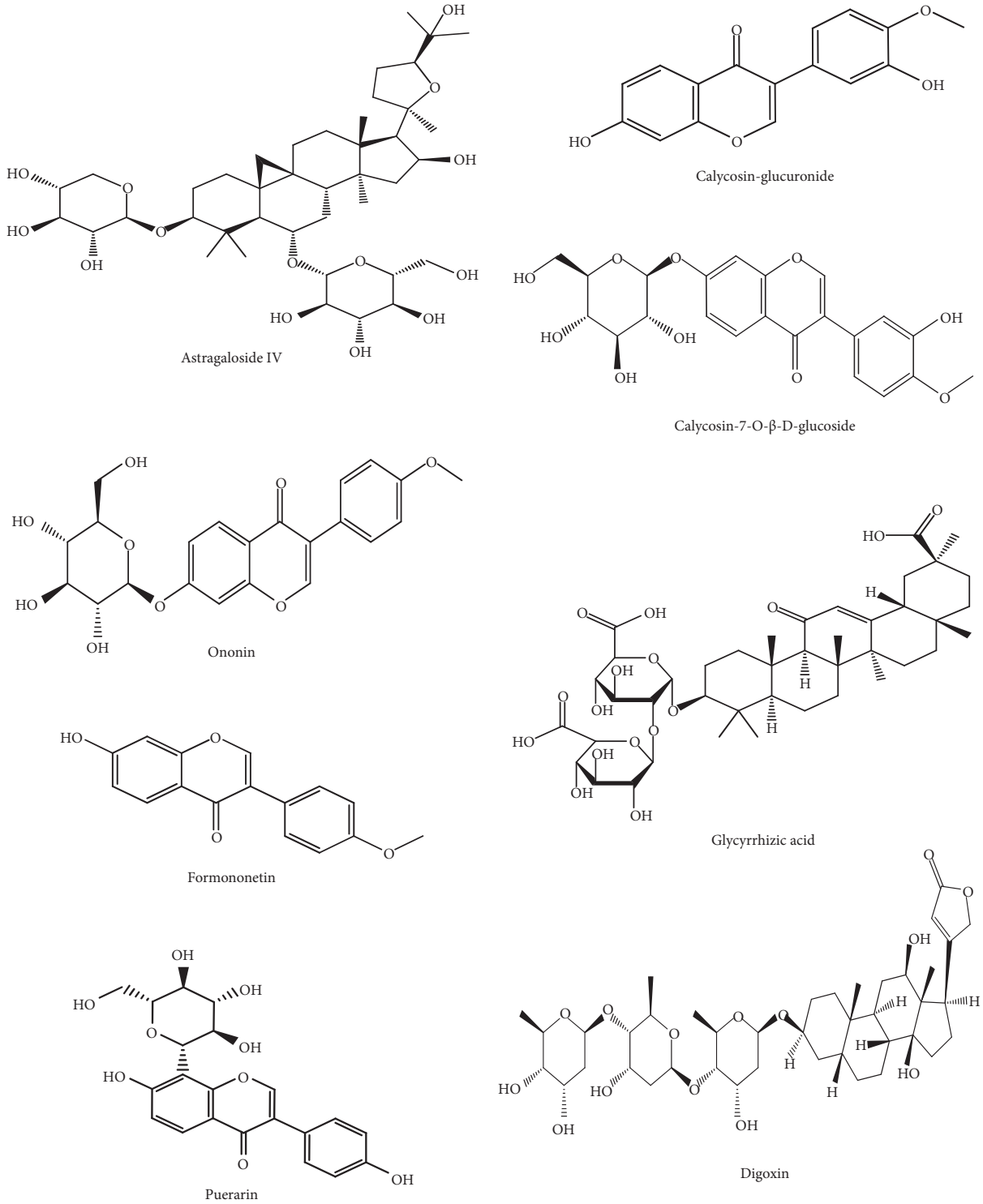


Figure 1: The chemical structure of six analytes.

Nevertheless, the major recipients of these drugs are patients. In a pathological state, the severity of the pathological state can have significant effects on the absorption, distribution, metabolism, and excretion of the drug, which is undeviatingly associated with the efficiency and side effects of the drug. The pharmacokinetic study of TCM under physiological and pathological conditions will support the rational application of TCMs in the clinic. Concerning the clinically safe medication of renal diseases, pharmacokinetic research about TCM can contribute more credible information, which helps significantly to elucidate the safety and effectiveness of drugs during the treatment process [12–14].

Previous reports have focused on the pharmacological effects of HQD while also encompassing some pharmacokinetic investigation. However, most pharmacokinetic studies of effective constituents of HQD to date have conducted

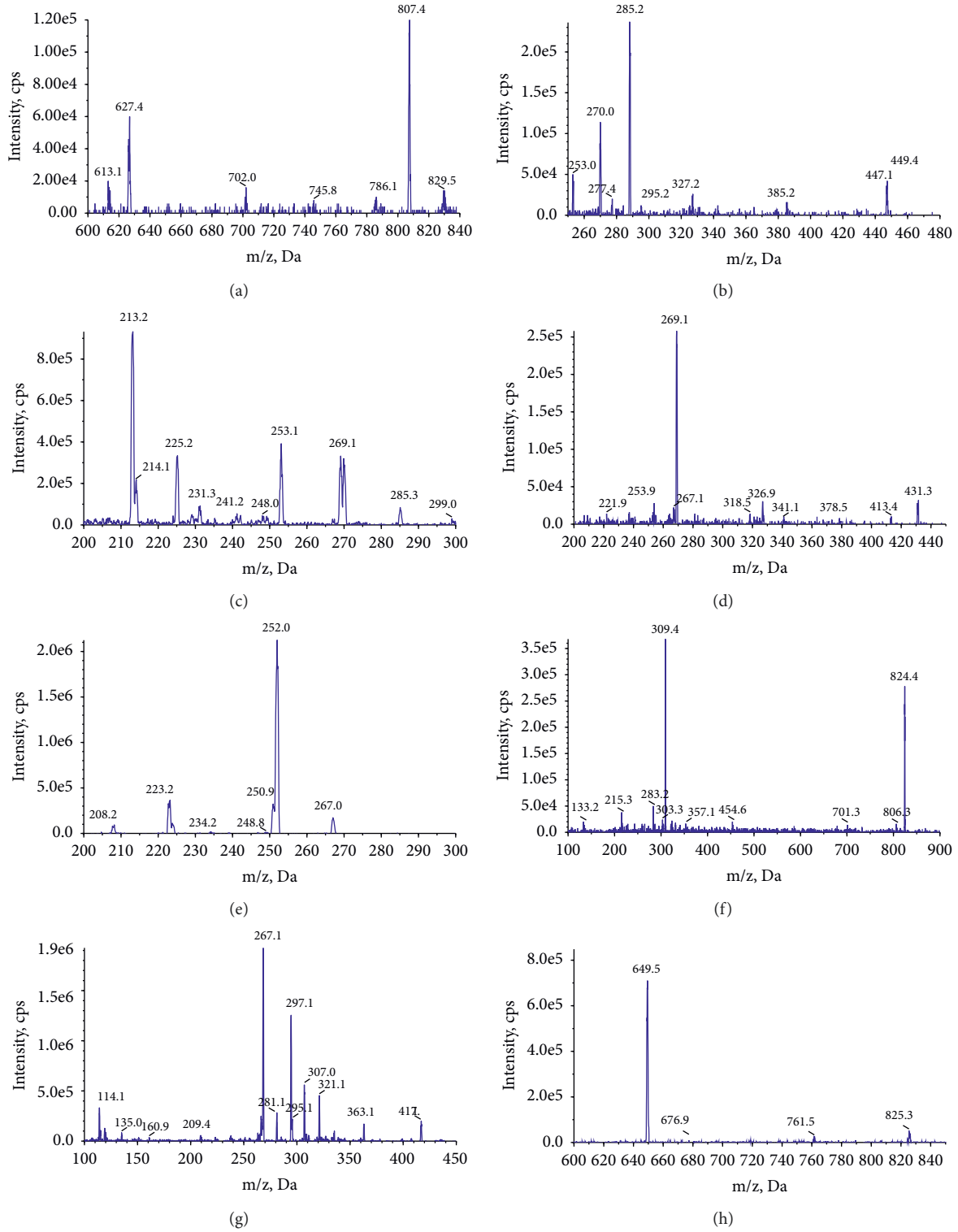


Figure 2: The mass spectra of six analytes. (a) Astragaloside IV, (b) calycosin-7-O-$\beta$-D-glucoside, (c) calycosin-glucuronide, (d) ononin, (e) formononetin, (f) glycyrrhetinic acid, (g) puerarin, and (h) digoxin.

their investigations under normal conditions. Based on the above reason, in this study, a high-performance liquid chromatography-tandem mass spectrometry (HPLC-MS/MS) method for the simultaneous determination of six active ingredients of HQD, including astragaloside IV, calycosin-7-O-$\beta$-D-glucoside, calycosin-glucuronide, ononin, formononetin, and glycyrrhizic acid in mouse plasma, was first established. Then, the pharmacokinetic differences of these six active ingredients were investigated between control and DN mice after the oral administration of HQD, which would provide some reference for the dose adjustment of HQD in clinic.

Table 1: The biochemical indicators of control and 12-week db/db mice ($\overline{x} \pm SD$, $n = 6$).

| Group | Blood glucose (mmol/L) | Serum creatinine ($\mu$mol/L) | Urea nitrogen (mmol/L) | Triglyceride (mmol/L) | Cholesterol (mmol/L) | 24 h urinary albumin (mg/day) |
|---|---|---|---|---|---|---|
| Control | $6.07 \pm 0.88$ | $22.84 \pm 5.29$ | $6.07 \pm 1.31$ | $0.96 \pm 0.19$ | $3.03 \pm 0.35$ | $17.34 \pm 1.36$ |
| db/db | $18.05 \pm 2.87^{**}$ | $31.49 \pm 5.76^{*}$ | $7.78 \pm 1.23^{*}$ | $1.79 \pm 0.27^{**}$ | $3.87 \pm 0.51^{**}$ | $28.44 \pm 3.17^{**}$ |

ps: vs. control group, $^{*}P < 0.05$, $^{**}P < 0.01$.

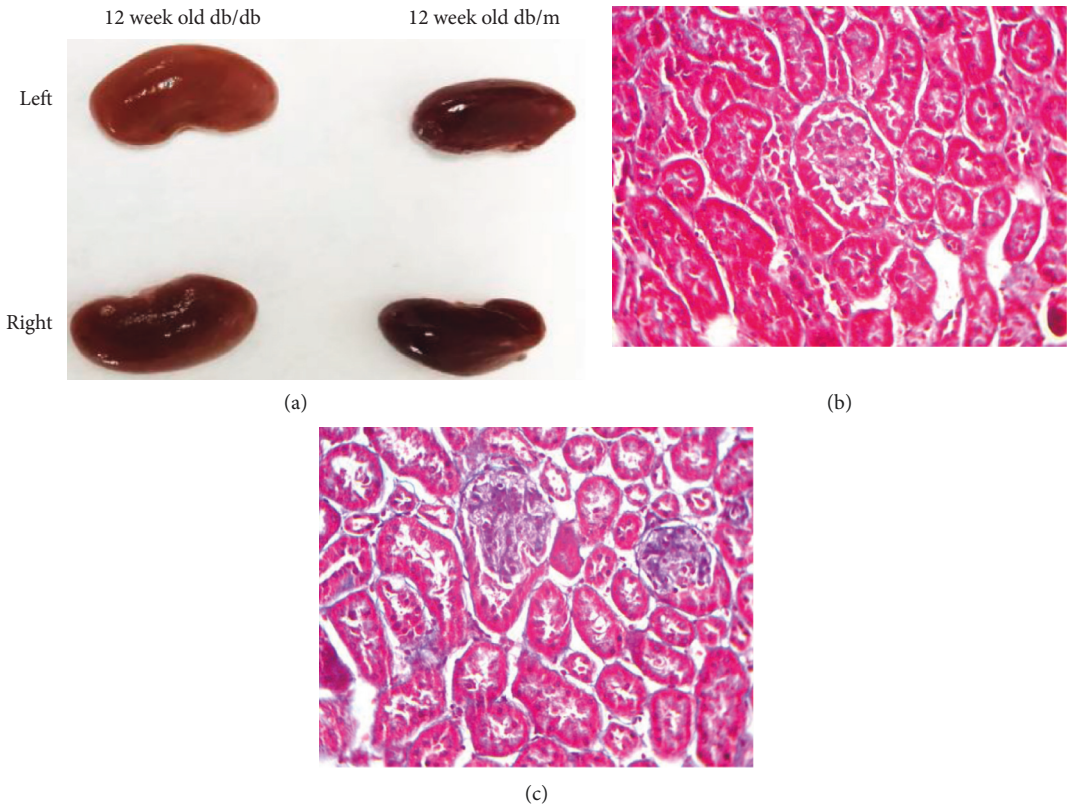


Figure 3: Observation of the shape of 12-week db/db and db/m control mice (a), renal pathological sectioning of db/m control mice (b), and renal pathological sectioning of 12-week db/db mice (c) (Masson, ×400).

## 2. Materials and Methods

*2.1. Materials.* The reference standards of astragaloside IV (purity >99.0%), calycosin-7-O-$\beta$-D-glucoside (purity >98.0%), calycosin-glucuronide (purity >98.0%), formononetin (purity >98.0%), ononin (purity >98.0%), glycyrrhetinic acid (purity >99.0%), puerarin (internal standard, IS, purity >98.0%), and digoxin (IS, purity >98.0%) were obtained from the National Institute for the Control of Pharmaceutical and Biological Products (Beijing, China). Acetonitrile and methanol (HPLC grade) were purchased from Merck KGaA (Darmstadt, Germany). Other chemicals used were of reagent grade or analytical grade.

A mixture of four active constituents from HQD was produced. The composition is as follows: astragalus saponin with a 72.04% content, which was 2.69% astragaloside IV; astragalus flavone with a 69.43% content, which was 1.62% calycosin-7-O-$\beta$-D-glucoside, 1.42% calycosin-glucuronide, 0.89% ononin, and 0.31% formononetin; glycyrrhetinic acid with a 72.04% content; and astragalus polysaccharides with a 65.82% content.

*2.2. Animals.* Ten-week-old db/db mice (weighing $45 \pm 5$ g) and db/m mice (weighing $20 \pm 2$ g) were obtained from the Model Animal Research Center of Nanjing University (Qualified number SCXK(Su)2018-0008) and raised in the specific-pathogen-free (SPF) laboratory of the Experimental Animal Center of Guizhou Medical University for two weeks. Ten-week-old db/db mice can develop nephropathy at 12 weeks of age. All mice were housed in polypropylene cages and maintained under standard conditions ($25^{\circ}C \pm 20^{\circ}C$; relative humidity, $60\% \pm 5\%$; and light-dark cycle of 12 h each). The protocols for all of the animal studies were approved by the Animal Ethics Committee of Guizhou Medical University (NO1702080).

*2.3. Conditions of HPLC-MS/MS.* Figure 1 shows the chemical structure of six analytes. An Acquity HPLC system (Shimadzu Corp., Kyoto, Japan) equipped with a Q-Trap® 5500 triple quadruple mass spectrometer (AB Sciex, Framingham, MA, USA) was employed for HPLC-MS/MS. The chromatographic conditions of the four constituents of HQD

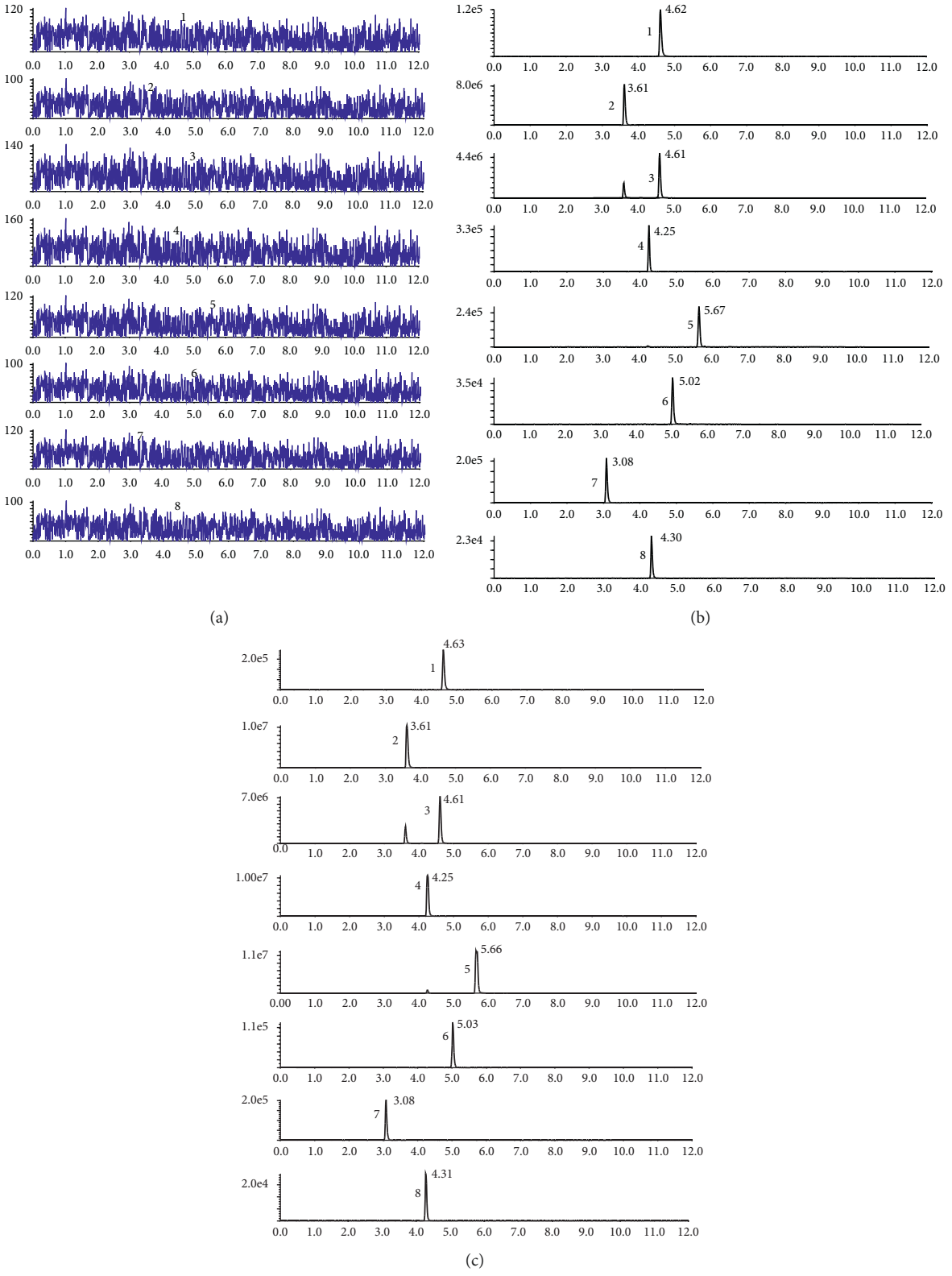


FIGURE 4: The chromatogram of HPLC-MS/MS. Blank plasma sample (a), blank plasma spiked with six ingredients and IS (b), and plasma samples obtained 30 min after oral HQD treatment (c).

were achieved on an Excel2C18-AR system (100 × 2.1 mm, 2 $\mu$m; Advanced Chromatography Technologies Ltd., Aberdeen, UK) maintained at 30°C. Analysis was completed with a gradient elution of 0.1% formic acid ($A$) and acetonitrile ($B$) and a flow rate of 0.4 mL/min. The gradient elution was as follows: 0 to 0.6 min (90% A), 0.6 to 2 min (90 ⟶ 70% $A$), 2 to 6 min (70 ⟶ 35% $A$), 6 to 8 min (35 ⟶ 10% $A$), 8 to 9 min (10 ⟶ 10% $A$), 9 to 9.1 min (10 ⟶ 90% $A$), and 9.1 to

Table 2: Calibration curve of six analytes in mouse plasma.

| Analyte | Linear regression equation | $r$ | Linear range (ng/mL) | LLOQ (ng/mL) | LOD (ng/mL) |
|---|---|---|---|---|---|
| Astragaloside IV | $Y = 0.0025X + 0.3926$ | 0.9993 | 10.68–2670 | 10.68 | 0.33 |
| Calycosin-7-O-$\beta$-D-glucoside | $Y = 0.0375X + 0.9606$ | 0.9995 | 5.05–505 | 5.05 | 0.01 |
| Calycosin-glucuronide | $Y = 0.0208X + 0.4845$ | 0.9995 | 5.19–2595 | 5.19 | 0.03 |
| Formononetin | $Y = 0.0043X + 0.1080$ | 0.9992 | 2.62–523 | 2.62 | 0.03 |
| Ononin | $Y = 0.0033X + 0.1591$ | 0.9990 | 5.07–1014 | 5.07 | 0.07 |
| Glycyrrhizic acid | $Y = 0.0109X + 0.5029$ | 0.9995 | 5.09–3817 | 5.09 | 0.04 |

Table 3: Intra- and interday precision and accuracy of six analytes in mouse plasma ($\overline{x} \pm$ SD, $n = 6$).

| Analyte | Concertation of analyte (ng/mL) | Mean ± SD (ng/mL) | Accuracy (%) | Interday precision RSD (%) | Intraday precision RSD (%) |
|---|---|---|---|---|---|
| Astragaloside IV | 16.02 | 15.01 ± 0.66 | 93.68 ± 6.71 | 4.42 | 8.47 |
| | 801 | 813.9 ± 74.06 | 101.6 ± 1.99 | 9.10 | 6.56 |
| | 1602 | 1522 ± 107.33 | 95.03 ± 7.20 | 7.05 | 7.08 |
| Calycosin-7-O-$\beta$-D-glucoside | 15.15 | 15.59 ± 1.55 | 102.9 ± 5.23 | 9.94 | 8.92 |
| | 75.75 | 67.65 ± 5.51 | 89.31 ± 7.56 | 8.14 | 5.39 |
| | 151.5 | 157.8 ± 5.67 | 104.2 ± 7.83 | 3.59 | 6.70 |
| Calycosin-glucuronide | 10.38 | 8.57 ± 0.48 | 82.57 ± 1.91 | 2.31 | 5.57 |
| | 519 | 492.9 ± 23.56 | 94.98 ± 9.15 | 4.78 | 6.10 |
| | 1038 | 927.5 ± 81.62 | 89.35 ± 7.03 | 8.80 | 5.27 |
| Formononetin | 5.23 | 5.02 ± 0.44 | 95.97 ± 8.32 | 8.67 | 6.41 |
| | 261.5 | 266.6 ± 19.86 | 101.9 ± 7.59 | 7.45 | 7.59 |
| | 313.8 | 307.4 ± 41.02 | 97.83 ± 10.18 | 13.35 | 7.10 |
| Ononin | 10.41 | 9.35 ± 0.77 | 92.24 ± 5.93 | 8.22 | 7.61 |
| | 507 | 445.8 ± 32.63 | 87.93 ± 5.11 | 7.32 | 10.16 |
| | 1014 | 1051 ± 60.94 | 103.6 ± 6.96 | 5.80 | 4.40 |
| Glycyrrhizic acid | 12.73 | 11.89 ± 1.3 | 93.40 ± 10.24 | 10.96 | 3.22 |
| | 1273 | 1046 ± 62.99 | 82.23 ± 1.34 | 1.62 | 5.28 |
| | 2545 | 2525 ± 142.15 | 99.21 ± 3.96 | 5.63 | 4.38 |

Table 4: Extraction recovery and matrix effect of six analytes in mouse plasma ($\overline{x} \pm$ SD, $n = 6$).

| Analyte | Concertation of analyte (ng/mL) | Extraction recovery (%) | RSD % | Matrix effect (%) | RSD % |
|---|---|---|---|---|---|
| Astragaloside IV | 16.02 | 99.78 ± 7.56 | 7.58 | 87.11 ± 6.52 | 7.48 |
| | 801 | 106.1 ± 8.53 | 8.04 | 94.20 ± 9.33 | 9.90 |
| | 1602 | 112.7 ± 6.14 | 5.44 | 85.36 ± 3.49 | 4.08 |
| Calycosin-7-O-$\beta$-D-glucoside | 15.15 | 91.18 ± 3.46 | 3.80 | 83.04 ± 2.79 | 3.35 |
| | 75.75 | 89.05 ± 9.37 | 10.52 | 90.46 ± 4.80 | 5.31 |
| | 151.5 | 94.7 ± 4.23 | 4.46 | 101.9 ± 6.78 | 6.65 |
| Calycosin-glucuronide | 10.38 | 96.56 ± 8.59 | 8.89 | 86.86 ± 4.76 | 5.48 |
| | 519 | 82.39 ± 1.27 | 1.54 | 107.90 ± 10.01 | 9.27 |
| | 1038 | 110.9 ± 7.38 | 6.66 | 91.45 ± 7.41 | 8.11 |
| Formononetin | 5.23 | 103.1 ± 8.40 | 8.15 | 90.86 ± 6.58 | 7.24 |
| | 261.5 | 88.54 ± 5.65 | 6.38 | 93.47 ± 7.60 | 8.13 |
| | 313.8 | 102.8 ± 9.73 | 9.47 | 99.22 ± 7.79 | 7.85 |
| Ononin | 10.41 | 87.28 ± 6.74 | 7.73 | 104.42 ± 10.60 | 10.15 |
| | 507 | 98.92 ± 11.01 | 11.13 | 85.95 ± 3.69 | 4.29 |
| | 1014 | 86.36 ± 4.19 | 4.85 | 103.38 ± 10.49 | 10.15 |
| Glycyrrhizic acid | 12.73 | 90.03 ± 7.80 | 8.66 | 83.77 ± 1.92 | 2.29 |
| | 1272.5 | 95.35 ± 7.06 | 7.41 | 93.47 ± 7.60 | 8.13 |
| | 2545 | 89.83 ± 4.29 | 4.78 | 99.22 ± 7.79 | 7.85 |

Table 5: Stability of six analytes in mouse plasma ($\overline{x} \pm SD$, $n = 6$).

| Analyte | Concertation of analyte (ng/mL) | Sampler 4 h | | −20°C 48 h | | Three freeze-thaw | |
|---|---|---|---|---|---|---|---|
| | | Mean ± SD (ng/mL) | RSD (%) | Mean ± SD (ng/mL) | RSD (%) | Mean ± SD (ng/mL) | RSD (%) |
| Astragaloside IV | 16.02 | 15.76 ± 1.34 | 8.52 | 15.17 ± 1.08 | 7.10 | 15.58 ± 1.58 | 10.14 |
| | 801 | 826.8 ± 49.36 | 5.97 | 841.1 ± 54.76 | 6.51 | 760.6 ± 50.89 | 6.69 |
| | 1602 | 1591 ± 113.94 | 7.16 | 1538 ± 62.14 | 4.04 | 1578 ± 72.92 | 4.62 |
| Calycosin-7-O-$\beta$-D-glucoside | 15.15 | 14.53 ± 0.93 | 6.40 | 14.72 ± 1.34 | 9.11 | 14.05 ± 1.31 | 9.31 |
| | 75.75 | 77.08 ± 4.93 | 6.39 | 82.83 ± 7.14 | 8.62 | 78.27 ± 2.88 | 3.68 |
| | 151.5 | 149.2 ± 10.29 | 6.90 | 143.8 ± 7.73 | 5.38 | 141.4 ± 9.57 | 6.77 |
| Calycosin-glucuronide | 10.38 | 9.99 ± 0.67 | 6.69 | 9.87 ± 0.34 | 3.42 | 9.71 ± 0.46 | 4.69 |
| | 519 | 523.5 ± 19.84 | 3.79 | 557.9 ± 50.32 | 9.02 | 532.1 ± 25.91 | 4.87 |
| | 1038 | 1025 ± 78.08 | 7.62 | 1031 ± 45.24 | 4.39 | 1051 ± 50.02 | 4.76 |
| Formononetin | 5.23 | 5.47 ± 0.57 | 10.89 | 5.58 ± 0.37 | 6.65 | 5.35 ± 0.63 | 11.73 |
| | 261.5 | 245.4 ± 1162.01 | 13.92 | 261.5 ± 23.25 | 8.89 | 251.2 ± 27.17 | 10.82 |
| | 313.8 | 311.6 ± 28.6 | 9.18 | 322.7 ± 30.69 | 9.51 | 308.7 ± 25.75 | 8.34 |
| Ononin | 10.41 | 9.67 ± 0.73 | 7.51 | 9.9 ± 0.46 | 4.63 | 9.79 ± 0.74 | 7.61 |
| | 507 | 505.7 ± 34.19 | 6.76 | 469.0 ± 41.13 | 8.77 | 475.6 ± 22.73 | 4.78 |
| | 1014 | 993.2 ± 66.94 | 6.74 | 942.6 ± 51.09 | 5.42 | 920.9 ± 40.52 | 4.40 |
| Glycyrrhizic acid | 12.73 | 11.64 ± 1.28 | 11.01 | 12.26 ± 0.77 | 6.27 | 11.89 ± 1.3 | 10.97 |
| | 1273 | 1250 ± 68.62 | 5.49 | 1186 ± 83.68 | 7.06 | 1185 ± 83.68 | 7.06 |
| | 2545 | 2472 ± 139.15 | 5.63 | 2463 ± 104.69 | 4.25 | 2414 ± 74.35 | 3.08 |

12 min (90% *A*). For MS/MS detection, an electrospray ionization in a multireaction monitoring mode was operated with polarity switching between negative and positive ion modes. The mass spectrometer parameters were set as follows: ion spray voltage at 5.5 kV (+) and −4.5 kV (−), source temperature at 600°C, nebulizer pressure at 55 psi, curtain gas at 30 psi, and auxiliary gas at 55 psi. The multiple reaction monitoring (MRM) analysis was conducted by monitoring the precursor ion to produce ion transitions of *m/z* 807.4 ⟶ 627.4 for astragaloside IV, 447.1 ⟶ 285.2 for calycosin-7-O-$\beta$-D-glucoside, 285.3 ⟶ 213.2 for calycosin-glucuronide, 267.0 ⟶ 252.0 for formononetin, 431.3 ⟶ 269.1 for ononin, 824.4 ⟶ 309.4 for glycyrrhizic acid, 417.1 ⟶ 267.1 for puerarin, and 825.3 ⟶ 649.5 for digoxin. Figure 2 shows the mass spectra of six analytes.

*2.4. Plasma Sample Preparation.* The whole blood samples were centrifuged at 4°C for 10 min at 3,000 rpm. A 50 $\mu$L aliquot of the supernatant was placed in the sample tubes and combined with 25 $\mu$L of methanoic acid (1 M), 25 $\mu$L of methanol, and 10 $\mu$L of internal standard solution (0.75 μg/mL of puerarin and 6.02 μg/mL of digoxin). Then, the mixture was added to 200 $\mu$L of methanol to be de-proteinated. Subsequently, the tubes were vortex-mixed for 5 min at 60 Hz and centrifuged for 10 min at 12,000 rpm. An aliquot of the upper organic layers was transferred to sample tubes and evaporated to dryness with a nitrogen-blowing instrument (Organomation, Berlin, MA, USA) at 40°C. The residue was sonicated with 50 $\mu$L of 50% methanol and then centrifuged for 10 min at 10,000 rpm. Then, 1 $\mu$L of supernatant was injected into the HPLC-MS/MS system for analysis.

*2.5. Preparation of Standard Samples.* Stock solutions were separately prepared by dissolving astragaloside IV (5.34 mg), calycosin-7-O-$\beta$-D-glucoside (5.05 mg), calycosin-glucuronide (5.19 mg), ononin (5.07 mg), formononetin (5.23 mg), and glycyrrhizic acid (5.09 mg) into methanol to yield the following concentrations: astragaloside IV (0.534 mg/mL), calycosin-7-O-$\beta$-D-glucoside (0.505 mg/mL), calycosin-glucuronide (0.519 mg/mL), ononin (0.507 mg/mL), formononetin (0.523 mg/mL), and glycyrrhizic acid (0.509 mg/mL). A series of working standard solutions were prepared by dilution of the stock solution with methanol. All the stock and working solutions were stored at 4°C and brought to room temperature before use. Quality control samples representing the low, medium, and high concentrations were separately prepared for each analyte.

*2.6. Method Validation*

*2.6.1. Specificity.* The blank plasma sample chromatogram was conducted under the method of plasma sample preparation using 50 $\mu$L of blank plasma taken from each mouse, except for adding IS. The blank plasma was spiked with astragaloside IV, calycosin-7-O-$\beta$-D-glucoside, calycosin-glucuronide, ononin, formononetin, and glycyrrhizic acid, and IS chromatogram, and plasma samples obtained after the oral administration of HQD were treated in the same fashion.

*2.6.2. Calibration Curves and Linearity.* The stock solution of astragaloside IV, calycosin-7-O-$\beta$-D-glucoside, calycosin-glucuronide, ononin, formononetin, and glycyrrhizic acid was closely weighed and added to methanol as desired for dilution to create a series of mixed working solutions. Calibration standards were prepared by spiking the appropriate standard working solutions with 50 $\mu$L of blank plasma to yield calibration concentrations of six analytes. The calibration curves were fitted using a weighted least-squares linearity regression. The calibration curves were

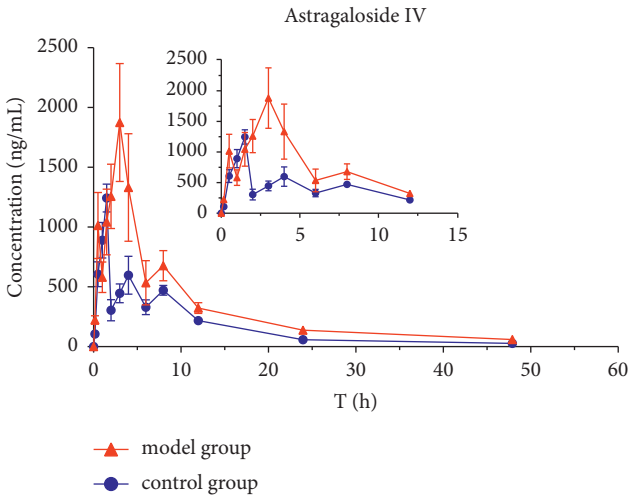


Figure 5: Concentration-time profiles of astragaloside IV after HQD administration ($\overline{x} \pm \mathrm{SD}$, $n = 8$).

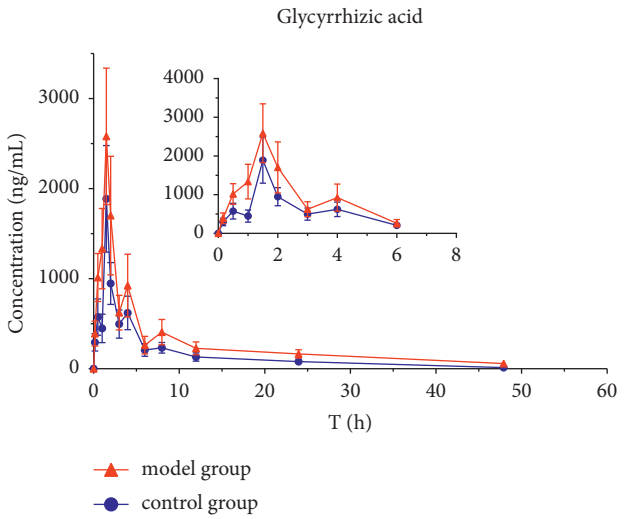


Figure 6: Concentration-time profiles of glycyrrhizic acid after HQD administration ($\overline{x} \pm \mathrm{SD}$, $n = 8$).

obtained by plotting the peak area ratio compared with the concentration of the six analytes with linear regression using standard plasma samples at seven concentrations.

*2.6.3. Accuracy and Precision.* The quality control samples at three concentration levels of six kinds of analytes of mouse plasma were prepared and operated in parallel according to the above methods of plasma sample preparation, with each concentration analyzed by six replicates. Assay precision was calculated by using the relative standard deviation (RSD, %) and variance. Accuracy was expressed as mean ± standard deviation.

*2.6.4. Extraction Efficiency and Matrix Effect.* Blank plasma solutions (50 $\mu$L) spiked with the quality control sample at

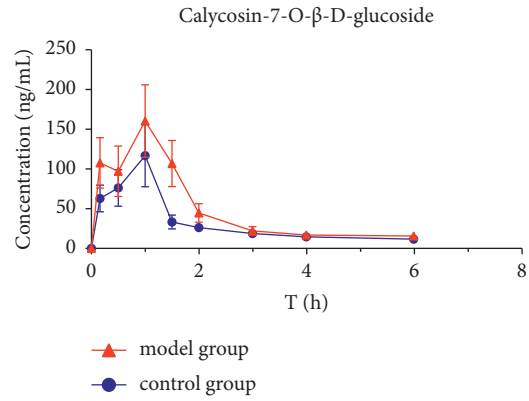


Figure 7: Concentration-time profiles of calycosin-7-O-$\beta$-D-glucoside after HQD administration ($\overline{x} \pm \mathrm{SD}$, $n = 8$).

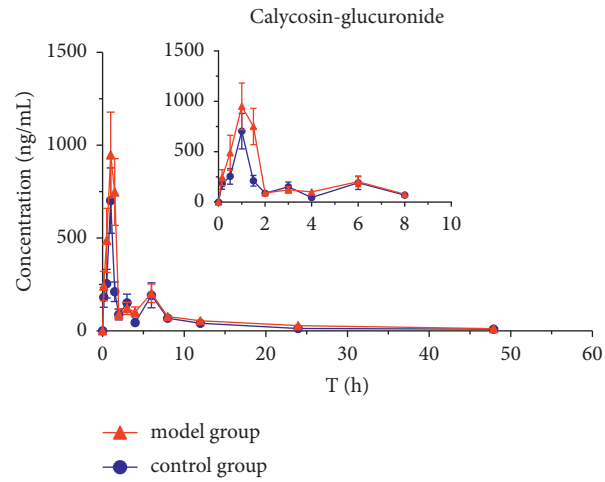


Figure 8: Concentration-time profiles of calycosin-glucoside after HQD administration ($\overline{x} \pm \mathrm{SD}$, $n = 8$).

three concentration levels (low, medium, and high), each with six replicates, were prepared according to the above methods of plasma sample preparation and regarded as sample *A*. Another 50 $\mu$L of blank plasma was prepared according to the above methods of plasma sample preparation, and sample *B* was obtained by mixing standard solution and IS into the obtained supernatant followed by evaporation. Then, the residue was reconstituted with 50 $\mu$L of methanol. Sample *C* was acquired by mixing standard solution and IS followed by evaporation. Then, the residue was reconstituted with 50 $\mu$L of methanol. Extraction efficiency was calculated by the peak area ratio (*A*/*B*), and the matrix effect was calculated by the peak area ratio (*B*/*C*).

*2.6.5. Stability.* Quality control samples at three concentrations of three kinds of constituents of mouse plasma were prepared to investigate the stability of six analytes of processed plasma samples After storing them at room temperature (approximately 25°C) for 24 hours, we froze them (−20°C) for 48 hours, and repeated freezing and thawing three times. They were then processed based on the

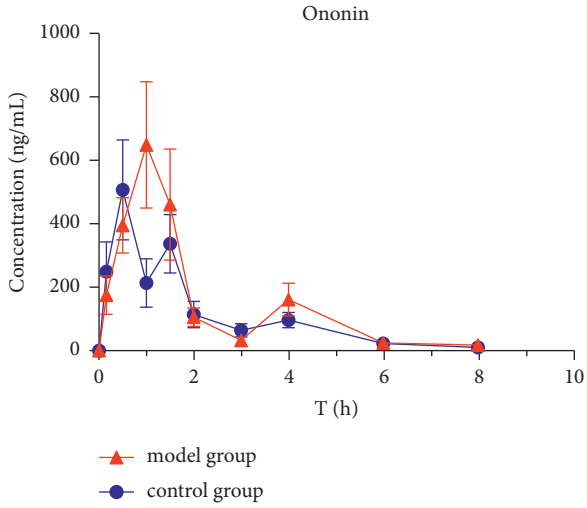


Figure 9: Concentration-time profiles of ononin after HQD administration ($\overline{x} \pm$ SD, $n = 8$).

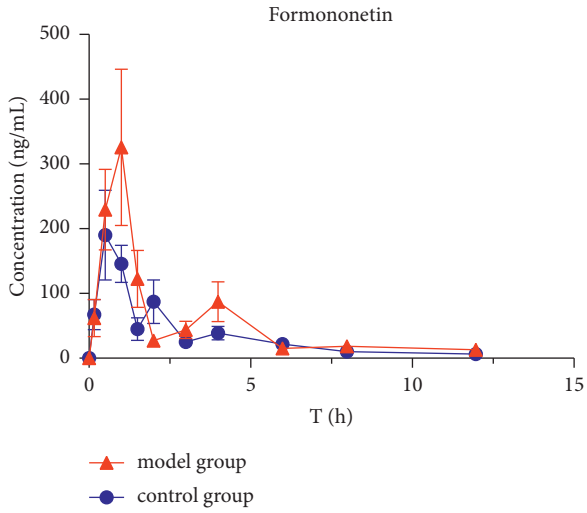


Figure 10: Concentration-time profiles of formononetin after HQD administration ($\overline{x} \pm$ SD, $n = 8$).

abovementioned plasma sample processing method and measured by HPLC-MS/MS.

*2.7. Pharmacokinetic Analysis.* The model and control mice were randomly divided into two groups. All mice were fasted overnight (12 h) prior to a single oral administration of HQD (1.64 g/kg), and 0.2 mL of blood was collected from the heart of each animal at 0, 10, and 30 min and 1, 1.5, 2, 3, 4, 6, 8, 12, 24, and 48 h. The blood concentration at each time point was the average value from eight mice. The pharmacokinetic parameters of six ingredients were calculated by WinNoLin version 6.4 using a noncompartment model. All of the data are presented as mean ± standard deviation values. Statistical analysis between the two groups was performed using SPSS version 23 (IBM Corporation, Armonk, NY, USA). $P \leq 0.01$ and $P \leq 0.05$ between the two groups were statistically different.

Table 6: The pharmacokinetic parameters of astragaloside IV after HQD administration.

| Pharmacokinetic parameter | Unit | Astragaloside IV | |
|---|---|---|---|
| | | Control group | Model group |
| $T_{1/2}$ | h | 9.85 ± 0.82 | 15.11 ± 1.15** |
| $T_{max}$ | h | 1.75 ± 0.29 | 2.75 ± 0.50* |
| $C_{max}$ | ng/mL | 1248 ± 101.7 | 1882 ± 429.1* |
| $AUC_{(0-t)}$ | ng*h/mL | 7624 ± 235.7 | 14414 ± 952.1** |
| $AUC_{(0-\infty)}$ | ng*h/mL | 8012 ± 266.8 | 15710 ± 895.4** |
| $V_Z/F$ | mL/kg | 191756 ± 1417 | 15025 ± 1133** |
| $CL_Z/F$ | mL/h/kg | 1351 ± 44.04 | 690.3 ± 39.31** |
| $MRT_{(0-t)}$ | h | 9.95 ± 0.47 | 10.49 ± 1.13 |
| $MRT_{(0-\infty)}$ | h | 12.44 ± 1.19 | 15.33 ± 1.60 |

ps: vs. control group, $^*P < 0.05$, $^{**}P < 0.01$.

Table 7: The pharmacokinetic parameters of glycyrrhizic acid after HQD administration ($\overline{x} \pm$ SD, $n = 8$).

| Pharmacokinetic parameter | Unit | Glycyrrhizic acid | |
|---|---|---|---|
| | | Control group | Model group |
| $T_{1/2}$ | h | 9.87 ± 1.64 | 17.78 ± 3.55* |
| $T_{max}$ | h | 1.38 ± 0.25 | 1.63 ± 0.25 |
| $C_{max}$ | ng/mL | 1892 ± 513.8 | 2661 ± 630.1 |
| $AUC_{(0-t)}$ | ng*h/mL | 6962 ± 729.8 | 12174 ± 1374** |
| $AUC_{(0-\infty)}$ | ng*h/mL | 7152 ± 725.4 | 13725 ± 1497** |
| $V_Z/F$ | mL/kg | 180200 ± 40486 | 169076 ± 38405 |
| $CL_Z/F$ | mL/h/kg | 12618 ± 1340 | 6590 ± 787.4** |
| $MRT_{(0-t)}$ | h | 9.12 ± 0.96 | 11.48 ± 1.71 |
| $MRT_{(0-\infty)}$ | h | 10.56 ± 0.45 | 18.49 ± 4.74* |

ps: vs. control group, $^*P < 0.05$, $^{**}P < 0.01$.

## 3. Results and Discussion

*3.1. Evaluation of the Animal Model.* Table 1 shows that the biochemical indicators of blood glucose, serum creatinine, blood urea nitrogen, and 24-hour urinary albumin were significantly increased ($P < 0.05$) in 12-week-old db/db mice. As compared to control mice, the kidneys of 12-week-old db/db mice were obviously enlarged and their surface was not smooth. Renal pathological sectioning revealed an obvious degree of collagen fiber (blue part) in the renal tubules and glomerular basement membrane of 12-week-old db/db mice. We concluded that diabetic db/db mice can develop DN at 12 weeks of age. Therefore, the 12-week db/db mice were used as the model group. The kidney shape and pathological sectioning of 12-week db/db and db/m control mice are seen in Figure 3.

The db/db mouse is a mutant-type mouse with a leptin receptor gene defect picked from C57BL/6J mice by the

Table 8: The pharmacokinetic parameters of calycosin-7-O-$\beta$-D-glucoside after HQD administration ($\overline{x} \pm$ SD, $n = 8$).

| Pharmacokinetic parameter | Unit | Calycosin-7-O-$\beta$-D-glucoside | |
|---|---|---|---|
| | | Control group | Model group |
| $T_{1/2}$ | h | 3.22 ± 0.88 | 3.85 ± 2.21 |
| $T_{max}$ | h | 1.13 ± 0.25 | 1.25 ± 0.29 |
| $C_{max}$ | ng/mL | 117.5 ± 34.19 | 161.2 ± 39.84 |
| $AUC_{(0-t)}$ | ng*h/mL | 118.3 ± 12.90 | 191.0 ± 15.68** |
| $AUC_{(0-\infty)}$ | ng*h/mL | 175.7 ± 22.75 | 273.9 ± 49.48* |
| $V_Z/F$ | mL/kg | 65898 ± 12674 | 48618 ± 20157 |
| $CL_Z/F$ | mL/h/kg | 14611 ± 2106 | 9473 ± 1511* |
| $MRT_{(0-t)}$ | h | 1.62 ± 0.21 | 1.37 ± 0.11 |
| $MRT_{(0-\infty)}$ | h | 4.27 ± 1.44 | 4.30 ± 1.90 |

ps: vs. control group, $^*P < 0.05$, $^{**}P < 0.01$.

Table 9: The pharmacokinetic parameters of calycosin-glucuronide after HQD administration ($\overline{x} \pm$ SD, $n = 8$).

| Pharmacokinetic parameter | Unit | Calycosin-glucoside | |
|---|---|---|---|
| | | Control group | Model group |
| $T_{1/2}$ | h | 13.16 ± 1.74 | 15.62 ± 1.50 |
| $T_{max}$ | h | 0.88 ± 0.25 | 1.13 ± 0.25 |
| $C_{max}$ | ng/mL | 704.6 ± 152.8 | 954.8 ± 194.7 |
| $AUC_{(0-t)}$ | ng*h/mL | 1851 ± 264.6 | 2701 ± 211.0** |
| $AUC_{(0-\infty)}$ | ng*h/mL | 2034 ± 265.9 | 2977 ± 218.1** |
| $V_Z/F$ | mL/kg | 21128 ± 4333 | 16877 ± 1939 |
| $CL_Z/F$ | mL/h/kg | 1110 ± 144.3 | 749.9 ± 55.07** |
| $MRT_{(0-t)}$ | h | 10.15 ± 0.32 | 10.47 ± 0.44 |
| $MRT_{(0-\infty)}$ | h | 15.27 ± 1.08 | 15.98 ± 1.87 |

ps: vs. control group, $^*P < 0.05$, $^{**}P < 0.01$.

Table 10: The pharmacokinetic parameters of ononin after HQD administration ($\overline{x} \pm$ SD, $n = 8$).

| Pharmacokinetic parameter | Unit | Ononin | |
|---|---|---|---|
| | | Control group | Model group |
| $T_{1/2}$ | h | 1.31 ± 0.02 | 1.63 ± 0.83 |
| $T_{max}$ | h | 1.38 ± 0.25 | 1.25 ± 0.29 |
| $C_{max}$ | ng/mL | 351.6 ± 63.44 | 677.4 ± 157.9* |
| $AUC_{(0-t)}$ | ng*h/mL | 576.0 ± 43.31 | 817.0 ± 93.25** |
| $AUC_{(0-\infty)}$ | ng*h/mL | 596.4 ± 44.22 | 865.9 ± 106.9** |
| $V_Z/F$ | mL/kg | 4434.7 ± 357.0 | 3739 ± 1618 |
| $CL_Z/F$ | mL/h/kg | 2343 ± 171.8 | 1633 ± 226.9** |
| $MRT_{(0-t)}$ | h | 1.80 ± 0.21 | 1.67 ± 0.14 |
| $MRT_{(0-\infty)}$ | h | 2.04 ± 0.27 | 2.14 ± 0.32 |

ps: vs. control group, $^*P < 0.05$, $^{**}P < 0.01$.

Table 11: The pharmacokinetic parameters of formononetin after HQD administration ($\overline{x} \pm$ SD, $n = 8$).

| Pharmacokinetic parameter | Unit | Formononetin | |
|---|---|---|---|
| | | Control group | Model group |
| $T_{1/2}$ | h | 3.17 ± 0.47 | 4.71 ± 1.17* |
| $T_{max}$ | h | 0.63 ± 0.25 | 0.75 ± 0.29 |
| $C_{max}$ | ng/mL | 191.1 ± 69.46 | 354.9 ± 74.35* |
| $AUC_{(0-t)}$ | ng*h/mL | 429.4 ± 24.92 | 645.03 ± 105.8** |
| $AUC_{(0-\infty)}$ | ng*h/mL | 460.1 ± 32.3 | 730.61 ± 88.31** |
| $V_Z/F$ | mL/kg | 4791.9 ± 346.9 | 4569 ± 1498 |
| $CL_Z/F$ | mL/h/kg | 1047 ± 76.97 | 664.3 ± 80.3** |
| $MRT_{(0-t)}$ | h | 2.92 ± 0.22 | 3.04 ± 0.28 |
| $MRT_{(0-\infty)}$ | h | 3.83 ± 0.39 | 4.96 ± 0.96 |

ps: vs. control group, $^*P < 0.05$, $^{**}P < 0.01$.

Jackson Laboratory of the United States. It has the features of spontaneously developed type 2 diabetes, and its pathogenesis is very similar to human type 2 diabetes. Db/db mice continuously experience obesity, hyperlipidemia, hyperglycemia, diabetes, and other diabetic symptoms after 4 weeks of age. Then, they began to experience DN after 8–12 weeks [15, 16]. The experimental results showed that the blood glucose, blood creatinine, urea nitrogen, triglycerides, cholesterol, and 24-h urine albumin of 12-week db/db mice were significantly higher than those of the normal control group ($P < 0.05$). The kidney pathological tissue sections of 12-week db/db mice had obvious glomerular and renal tubular lesions. In this case, this experiment used 12-week db/db mice as the DN mouse model, including same-week-old db/m mice as the normal comparison group.

*3.2. Method Validation.* Currently, the commonly applied plasma sample-processing methods principally include solid-phase extraction, liquid-liquid extraction, organic solution protein precipitation, and multiple processing methods [17]. Based on the duality and solubility of saponins and flavonoids examined in this experiment, protein precipitation agents such as methanol, acetonitrile, and ethyl acetate, including the extraction method with *n*-butanol, were examined in the study. The methanol was used as the protein precipitation solvent for the experimental samples. We reviewed 1×, 2×, and 4× methanol as the protein precipitant. When 4× methanol was used as the protein precipitant, the separation of the ingredients was good. Furthermore, the recovery rate could meet the analysis requirements of biological samples. Meanwhile, combining an appropriate amount of formic acid when precipitating proteins with methanol can significantly enhance the recovery rate. The final resolution of the plasma sample-processing method is to acidify the plasma with 1% formic

acid solution, then attach methanol to the vortex, and mix for protein precipitation.

There are various types of TCMs, with numerous components and complex structures, including a low oral bioavailability. The triple quadrupole mass spectrometer has the advantages of a short analysis time, accurate quantification, and the capacity to examine many components. Currently, it is the most illustrative quantitative analysis instrument in the area of mass spectrometry, and it has been widely used in the pharmacokinetics of multicomponent TCMs [18, 19]. An HPLC-MS/MS method was established to concurrently determine astragaloside IV, calycosin-7-O-$\beta$-D-glucoside, calycosin-glucuronide, ononin, formononetin, and glycyrrhizic acid in mouse plasma. Additionally, digoxin was chosen as the internal standard substance identified in the negative ion mode. There is no mutual interference with endogenous substances in plasma, which can have a better correction impact. According to the nature of the mixture, methanol/water is used as the liquid mobile phase and 0.1% formic acid is attached to decrease peak tailing and improve the symmetry of the chromatographic peak. Eventually, the chromatographic column ACEExcel2C18-AR (1100 × 2.1 mm, 2 $\mu$m; Advanced Chromatography Technologies Ltd., Aberdeen, Scotland) was used. The column temperature was 30°C, and the volume flow was 0.4 mL/min. Moreover, the mobile phase was *A* (water, 0.1% formic acid aqueous solution) and *B* (acetonitrile) gradient elution as HPLC liquid-phase separation conditions. Methodologically confirmed, the method has high sensitivity, good repeatability, accurate results, and high specificity and meets the requirements of biological sample examination and detection.

*3.2.1. Specificity.* For the chromatograms of the blank plasma sample, the blank plasma spiked with astragaloside IV (1), calycosin-7-O-$\beta$-D-glucoside (2), calycosin-glucuronide (3), ononin (4), formononetin (5), and glycyrrhizic acid (6), and IS (puerarin and digoxin), and plasma samples obtained after oral administration of HQD are displayed in Figure 4. The results indicated that good separation was observed among the analytes, and no interference from the endogenous substances interfered with the determination of analyte and IS.

*3.2.2. Calibration Curves and Linearity.* The typical equation of linearity ranges and calibration curves for the six analytes are shown in Table 2. The results show that all the correlation coefficients were >0.99, indicating that the concentrations of the six analytes of astragaloside IV, calycosin-7-O-$\beta$-D-glucoside, calycosin-glucuronide, ononin, formononetin, and glycyrrhizic acid in mouse plasma correlated well within the linearity ranges.

*3.2.3. Accuracy and Precision.* The results of the intra- and interday precision and accuracy of six analytes in plasma samples are shown in Table 3. The RSD (%) values of intra- and interday precision for all analytes were ≤15%, and the RSD (%) values of accuracy of six analytes were within the range of 81.22%–106.01%, These data suggest that both the precision and accuracy achieved with this method were accurate and reliable, with good repeatability.

*3.2.4. Extraction Efficiency and Matrix Effect.* The results of the extraction efficiency and matrix effect are shown in Table 4. The extraction efficiency and matrix effect of six analytes at three different concentrations and IS were found to be 82.04%–112.7%, which indicated that the recoveries of the six analytes were precise, consistent, and reproducible at different concentration levels in various plasma biosamples with no significant plasma matrix interference.

*3.2.5. Stability.* The results of stability are shown in Table 5. The stability test results indicated that the plasma samples had good stability under the three different conditions with a 10% concentration variation compared with the initial values.

*3.3. Pharmacokinetics of Six Active Ingredients in HQD.* The mean plasma concentration-time profiles ($n = 8$) of six active ingredients (astragaloside IV, calycosin-7-O-$\beta$-D-glucoside, calycosin-glucuronide, ononin, formononetin, and glycyrrhizic acid) after the oral administration of HQD are shown in Figures 5–10. The pharmacokinetic parameters of the six active ingredients are listed in Tables 6–11. The HPLC-MS/MS method was successfully applied to determine the pharmacokinetics of six active ingredients in the plasma of normal and DN mice after a single oral administration of HQD (1.64 g/kg). Following the oral administration of HQD, the area under the curve of six active ingredients (astragaloside IV, calycosin-7-O-$\beta$-D-glucoside, calycosin-glucuronide, ononin, formononetin, and glycyrrhizic acid) and the $C_{max}$ values of astragaloside IV, ononin, and formononetin in the model group were increased ($P < 0.05$), while $CL_Z/F$ had slowed down ($P < 0.05$). However, the $T_{1/2}$ of astragaloside IV, glycyrrhizic acid, and formononetin, and the MRT of glycyrrhizic acid and the $T_{max}$ of astragaloside IV in the model group were postponed ($P < 0.05$), while the $V_Z/F$ of astragaloside IV in the model group was slowed down ($P < 0.05$). There was no significant difference in other pharmacokinetic parameters.

A sensitive, accurate, and rapid HPLC-MS/MS method was developed and validated for the simultaneous quantification of six ingredients of HQD in mouse plasma. Following the oral administration of HQD, the blood concentration level of ononin was lower than the detection line at 8 h, and the blood concentration level of calycosin-7-O-$\beta$-D-glucoside was lower than the detection line at 6 h. Glucoside was contained in the structure of flavonoids, which are easily metabolized using bacteria after entering the intestine [20, 21]. Meanwhile, calycosin-7-O-$\beta$-D-glucoside and formononetin were rapidly metabolized into aglycones due to the actions of bacteria in the intestine, resulting in a shortened retention time of the prototype in the body. The mean plasma concentration-time profiles of six components

both appeared to have multiple peaks, which could be explained as a phenomenon in two ways. On the one hand, drugs discharged through bile into the intestine can be reabsorbed through the portal vein into the bloodstream. On the other hand, the drug may be absorbed at multiple sites, and interactions with other medications could also cause its blood concentration level to rise again.

Within the HQD, the pharmacokinetic parameters of astragaloside IV, calycosin-7-O-$\beta$-D-glucoside, calycosin-glucuronide, ononin, formononetin, and glycyrrhizic acid have meaningful diversity in physiological and pathological conditions. Then, in contrast to normal mice, the absorption of six index components in DN mice significantly increased. Their metabolism and elimination were slowed down, and the retention time in the body was imperceptibly longer. This may be because of a modification in the activity or expression of many drug-metabolizing enzymes and transporters implicated in drug absorption and metabolism in the stage of DN that leads to changes in drug absorption and metabolic processes in the body. The kidneys are important secretion and excretion organs of the body. Apart from drugs eliminated by the liver and gallbladder, most drugs are excreted by the kidneys in their original form or as metabolites. The excretion of drugs is the result of the combined effects of nephron filtration, secretion, and reabsorption [22–24]. Consequently, the impairment of renal function may also be one of the reasons for the slowing down of drug elimination.

## 4. Conclusions

We have developed a sensitive and reliable HPLC-MS/MS method for simultaneous quantitation of astragaloside IV, calycosin-7-O-$\beta$-D-glucoside, calycosin-glucuronide, ononin, formononetin, and glycyrrhizic acid, which are the main active constituents in HQD, and compared the pharmacokinetics of these six active ingredients in control and DN mice orally treated with HQD.

## Data Availability

The data used to support the finding of this study are included within the article.

## Conflicts of Interest

The authors declare that there are no conflicts of interest regarding the publication of this article.

## Authors' Contributions

Qun Wang and Ya Shi authors contributed equally to this work. Qun Wang, Wen Liu, Yonglin Wang, and Zipeng Gong conceived and designed the experiments. Qun Wang and Ya Shi performed all of the experiments. Yonglin Wang, Ting Liu, Ya Shi, Yongjun Li, Xinli Song, Xiaolan Chen, and Yang Jin contributed to the operation of rats/reagents/materials/analysis tools. Qun Wang and Ya Shi analyzed the data. Qun Wang and Ya Shi wrote a draft of the manuscript. Wen Liu and Zipeng Gong contributed to critical review of the article.

## Acknowledgments

This research was supported by the First-Class Discipline Construction Project in Guizhou Province of China (GNYL (2017) 008), the Guizhou Characteristic Functional Food and TCM Preparation Development Platform KY[2020]006, the National Natural Science Foundation of China (No. 82060704 and No. 81860706), and the Project of Guizhou Provincial Department of Education (No. QJHKYZ[2022] 257).

## References

[1] Z. H. Zhang, J. R. Mao, H. Chen et al., "Removal of uremic retention products by hemodialysis is coupled with indiscriminate loss of vital metabolites," *Clinical Biochemistry*, vol. 50, no. 18, pp. 1078–1086, 2017.

[2] X. Y. Xiao, B. Ma, B. J. Dong et al., "Cellular and humoral immune responses in the early stages of diabetic nephropathy in NOD mice," *Journal of Autoimmunity*, vol. 32, no. 2, pp. 85–93, 2009.

[3] J. Kopel, C. Pena-Hernandez, and K. Nugent, "Evolving spectrum of diabetic nephropathy," *World Journal of Diabetes*, vol. 10, no. 5, pp. 269–279, 2019.

[4] H. Chen, L. Chen, D. Liu et al., "Combined clinical phenotype and lipidomic analysis reveals the impact of chronic kidney disease on lipid metabolism," *Journal of Proteome Research*, vol. 16, no. 4, pp. 1566–1578, 2017.

[5] R. Correa-Rotter and L. Gonzalez-Michaca, "Early detection and prevention of diabetic nephropathy: a challenge calling for mandatory action for mexico and the developing world," *Kidney International*, vol. 68, no. 98, pp. S69–S75, 2005.

[6] Y. b. Peng, D. Ren, Y. f. Song et al., "Effects of a combined fucoidan and traditional Chinese medicine formula on hyperglycaemia and diabetic nephropathy in a type II diabetes mellitus rat model," *International Journal of Biological Macromolecules*, vol. 147, pp. 408–419, 2020.

[7] X. Shi, X. G. Lu, L. B. Zhan et al., "The effects of the Chinese medicine ZiBu PiYin recipe on the hippocampus in a rat model of diabetes-associated cognitive decline: a proteomic analysis," *Diabetologia*, vol. 54, no. 7, pp. 1888–1899, 2011.

[8] G. D. Sun, C. Y. Li, W. P. Cui et al., "Review of herbal traditional Chinese medicine for the treatment of diabetic nephropathy," *Journal of Diabetes Research*, vol. 2016, Article ID 5749857, 18 pages, 2016.

[9] Y. L. Xu, Y. J. Zheng, and Z. Li, "Effect of Huangqi Liuyi Tang on glucose re-absorption via renal tubular epithelial cells in type 2 diabetes model rats," *Chinese Journal of Experimental Traditional Medical Formulae*, vol. 23, no. 11, pp. 114–121, 2017.

[10] L. M. Wen, Y. L. Xu, and Z. Li, "Study on the effects and mechanism of astragalus Liuyi Decoction on type 2 diabetes mellitus rats," *Journal of Chinese Medicinal Materials*, vol. 41, no. 3, pp. 699–702, 2018.

[11] Z. P. Gong, Y. Chen, R. J. Zhang, Q. Yang, and Xx. Zhu, "Advances on pharmacokinetics of traditional Chinese medicine under disease states," *China Journal of Chinese Materia Medica*, vol. 40, no. 2, pp. 169–173, 2015.

[12] S. Y. Zhu, X. Wang, Z. Zheng, X. E. Zhao, Y. Bai, and H. Liu, "Synchronous measuring of triptolide changes in rat brain

and blood and its application to a comparative pharmacokinetic study in normal and Alzheimer's disease rats," *Journal of Pharmaceutical and Biomedical Analysis*, vol. 185, Article ID 113263, 2020.

[13] W. Zhang, Z. T. Fu, Y. D. Xie, Z. W. Duan, Y. Wang, and R. H. Fan, "High resolution UPLC-MS/MS method for simultaneous separation and determination of six flavonoids from *semen cuscutae* extract in rat plasma: application to comparative pharmacokinetic studies in normal and kidney-deficient rats," *Natural Product Research*, vol. 34, no. 10, pp. 1446–1451, 2020.

[14] X. X. Dai, S. L. Su, H. D. Cai et al., "Comparative pharmacokinetics of acteoside from total glycoside extracted from leaves of rehmannia and dihuangye total glycoside capsule in normal and diabetic nephropathy rats," *Biomedical Chromatography*, vol. 31, no. 12, Article ID e4013, 2017.

[15] G. Appel, "Detecting and controlling diabetic nephropathy: what do we know," *Cleveland Clinic Journal of Medicine*, vol. 80, no. 4, pp. 209–217, 2013.

[16] C. Ponchiardi, M. Mauer, and B. Najafian, "Temporal profile of diabetic nephropathy pathologic changes," *Current Diabetes Reports*, vol. 13, no. 4, pp. 592–599, 2013.

[17] J. C. Dong, L. X. Zeng, and X. Wang, "Progress on application of biological sample pretreatment technology in pharmacokinetic research," *Traditional Chinese Drug Research and Clinical Pharmacology*, vol. 29, no. 1, pp. 110–117, 2018.

[18] H. Bo, R. H. Zhang, and X. H. Wang, "The application progress of triple quadrupole mass spectrometry in studies of traditional Chinese medicine," *Journal of Inner Mongolia University for Nationalities*, vol. 33, no. 3, pp. 208–212, 2018.

[19] X. Y. Liu, X. Y. Chen, and D. Y. Zhong, "Matrix effects and countermeasure of liquid chromatography-tandem mass spectrometry in bioanalysis," *Journal of Chinese Mass Spectrometry Society*, vol. 38, no. 4, pp. 388–399, 2017.

[20] L. Liu, X. L. Zhao, and L. Q. Di, "Effects of radix saposhnikoviae on metabolism of calycosin-7-O-$\beta$-D-glucoside in radix astragali by intestinal flora experiment in vitro," *Journal of Nanjing University of Traditional Chinese Medicine*, vol. 31, no. 2, pp. 170–173, 2015.

[21] W. Zhang, S. Jiang, D. W. Qian et al., "The interaction between ononin and human intestinal bacteria," *Acta Pharmaceutica Sinica*, vol. 49, no. 8, pp. 1162–1168, 2014.

[22] L. N. Wang, X. Lin, and L. Shen, "Effect of common clinical diseases on pharmacokinetics of traditional Chinese medicine," *Chinese Journal of Experimental Traditional Medical Formulae*, vol. 21, no. 18, pp. 206–210, 2015.

[23] G. l. Sun and X. Lin, "Mechanisms and strategies for targeting drugs to myocardial ischemic regions," *Acta Pharmaceutica Sinica*, vol. 45, no. 7, pp. 827–832, 2010.

[24] V. Pichette and F. A. Leblond, "Drug metabolism in chronic renal failure," *Current Drug Metabolism*, vol. 4, no. 2, pp. 91–103, 2003.